

# Search for alpha decay of naturally occurring osmium nuclides accompanied by gamma quanta

P. Belli<sup>a,b</sup>, R. Bernabei<sup>a,b,1</sup>, F. Cappella<sup>c,d</sup>, V. Caracciolo<sup>a,b,e</sup>, R. Cerulli<sup>a,b</sup>,  
 F.A. Danevich<sup>f</sup>, A. Incicchitti<sup>c,d</sup>, D.V. Kasperovych<sup>f</sup>, V.V. Kobychhev<sup>f</sup>,  
 G.P. Kovtun<sup>g,h</sup>, N.G. Kovtun<sup>g</sup>, M. Laubenstein<sup>e</sup>, D.V. Poda<sup>i</sup>, O.G. Polischuk<sup>f</sup>,  
 A.P. Shcherban<sup>g</sup>, S. Tessalina<sup>j</sup>, V.I. Tretyak<sup>f</sup>

<sup>a</sup>INFN, sezione Roma “Tor Vergata”, I-00133 Rome, Italy

<sup>b</sup>Dipartimento di Fisica, Università di Roma “Tor Vergata, I-00133 Rome, Italy”

<sup>c</sup>INFN, sezione Roma “La Sapienza”, I-00185 Rome, Italy

<sup>d</sup>Dipartimento di Fisica, Università di Roma “La Sapienza”, I-00185 Rome, Italy

<sup>e</sup>INFN, Laboratori Nazionali del Gran Sasso, 67100 Assergi (AQ), Italy

<sup>f</sup>Institute for Nuclear Research of NASU, 03028 Kyiv, Ukraine

<sup>g</sup>National Science Center “Kharkiv Institute of Physics and Technology”, 61108 Kharkiv, Ukraine

<sup>h</sup>Karazin Kharkiv National University, 4, 61022 Kharkiv, Ukraine

<sup>i</sup>Université Paris-Saclay, CNRS/IN2P3, IJCLab, 91405 Orsay, France

<sup>j</sup>John de Laeter Centre for Isotope Research, GPO Box U 1987, Curtin University, Bentley, WA, Australia

## Abstract

A search for  $\alpha$  decay of naturally occurring osmium isotopes to the lowest excited levels of daughter nuclei has been performed by using an ultra-low-background Broad-Energy Germanium  $\gamma$ -detector with a volume of 112 cm<sup>3</sup> and an ultra-pure osmium sample with a mass of 118 g at the Gran Sasso National Laboratory of the INFN (Italy). The isotopic composition of the osmium sample has been measured with high precision using Negative Thermal Ionisation Mass Spectrometry. After 15851 h of data taking with the  $\gamma$ -detector no effect has been detected, and lower limits on the  $\alpha$  decays were set at level of  $\lim T_{1/2} \sim 10^{15} - 10^{19}$  yr. The limits for the  $\alpha$  decays of <sup>184</sup>Os and <sup>186</sup>Os to the first excited levels of daughter nuclei,  $T_{1/2}(\text{<sup>184</sup>Os}) \geq 6.8 \times 10^{15}$  yr and  $T_{1/2}(\text{<sup>186</sup>Os}) \geq 3.3 \times 10^{17}$  yr (at 90% C.L.), exceed the present theoretical estimates of the decays half-lives. For <sup>189</sup>Os and <sup>192</sup>Os also decays to the ground states of the daughter nuclei were searched for due to the instability of the daughter nuclides relative to  $\beta$  decay.

*Keywords:* Alpha decay; <sup>184</sup>Os; <sup>186</sup>Os; <sup>187</sup>Os; <sup>188</sup>Os; <sup>189</sup>Os; <sup>190</sup>Os; <sup>192</sup>Os; Low-background HPGe  $\gamma$  spectrometry

## 1 Introduction

The interest to  $\alpha$  decay, a phenomenon discovered more than 100 years ago [1], is still great, both from the theoretical and the experimental sides. Various theoretical models are continuously

<sup>1</sup>Corresponding author at: Dipartimento di Fisica, Università di Roma “Tor Vergata”, I-00133 Rome, Italy. E-mail address: rita.bernabei@roma2.infn.it (R. Bernabei)

Table 1: Characteristics of  $\alpha$  decays of naturally occurring osmium isotopes.  $J^\pi$  is spin and parity of the nuclei,  $E$  is the energy of excited levels of the daughter nuclei, the  $Q_\alpha$  value is given for the g.s. to g.s. transitions. The g.s. of the parent nuclei is assumed. The limits obtained in the present work are given at 90% confidence level (C.L.).

Transition, $J^\pi$ , $E$ (keV)	$Q_\alpha$ (keV) [22]	Partial $T_{1/2}$ (yr)				Experimental
		[23]	[24, 25]	Theoretical [5]	[11]	
$^{184}\text{Os}, 0^+ \rightarrow ^{180}\text{W}, 0^+, \text{g.s.}$	2958.7(16)	$7.2 \times 10^{13}$	$3.5 \times 10^{13}$	$3.3 \times 10^{13}$	$2.1 \times 10^{13}$	$> 2.0 \times 10^{13}$ [17] $> 5.6 \times 10^{13}$ [19] $= (1.1 \pm 0.2) \times 10^{13}$ [20]
$^{184}\text{Os}, 0^+ \rightarrow ^{180}\text{W}, 2^+, 103.6$		$2.9 \times 10^{15}$	$1.3 \times 10^{15}$	$6.3 \times 10^{14}$	$7.3 \times 10^{14}$	$\geq 6.8 \times 10^{15}$ this work
$^{184}\text{Os}, 0^+ \rightarrow ^{180}\text{W}, 4^+, 337.6$		$2.5 \times 10^{19}$	$1.0 \times 10^{19}$	$9.2 \times 10^{17}$	$4.6 \times 10^{18}$	$\geq 4.6 \times 10^{16}$ this work
$^{186}\text{Os}, 0^+ \rightarrow ^{182}\text{W}, 0^+, \text{g.s.}$	2821.2(9)	$4.7 \times 10^{15}$	$1.9 \times 10^{15}$	$1.6 \times 10^{15}$	$1.0 \times 10^{15}$	$= (2.0 \pm 1.1) \times 10^{15}$ [21]
$^{186}\text{Os}, 0^+ \rightarrow ^{182}\text{W}, 2^+, 100.1$		$2.2 \times 10^{17}$	$8.3 \times 10^{16}$	$3.3 \times 10^{16}$	$3.9 \times 10^{16}$	$\geq 3.3 \times 10^{17}$ this work
$^{186}\text{Os}, 0^+ \rightarrow ^{182}\text{W}, 4^+, 329.4$		$2.9 \times 10^{21}$	$9.7 \times 10^{20}$	$7.2 \times 10^{19}$	$3.7 \times 10^{20}$	$\geq 6.0 \times 10^{18}$ this work
$^{187}\text{Os}, 1/2^- \rightarrow ^{183}\text{W}, 1/2^-, \text{g.s.}$	2721.7(9)	$4.5 \times 10^{19}$	$4.1 \times 10^{16}$	$5.1 \times 10^{16}$	$2.0 \times 10^{16}$	–
$^{187}\text{Os}, 1/2^- \rightarrow ^{183}\text{W}, 3/2^-, 46.5$		$4.4 \times 10^{20}$	$3.6 \times 10^{17}$	$6.7 \times 10^{18}$	$1.6 \times 10^{17}$	$\geq 3.2 \times 10^{15}$ this work
$^{187}\text{Os}, 1/2^- \rightarrow ^{183}\text{W}, 5/2^-, 99.1$		$2.8 \times 10^{21}$	$2.1 \times 10^{18}$	$4.0 \times 10^{19}$	$9.1 \times 10^{17}$	$\geq 1.9 \times 10^{17}$ this work
$^{188}\text{Os}, 0^+ \rightarrow ^{184}\text{W}, 0^+, \text{g.s.}$	2143.2(9)	$6.8 \times 10^{26}$	$1.4 \times 10^{26}$	$7.2 \times 10^{25}$	$5.2 \times 10^{25}$	–
$^{188}\text{Os}, 0^+ \rightarrow ^{184}\text{W}, 2^+, 111.2$		$2.9 \times 10^{29}$	$5.5 \times 10^{28}$	$1.3 \times 10^{28}$		$\geq 3.3 \times 10^{18}$ this work
$^{188}\text{Os}, 0^+ \rightarrow ^{184}\text{W}, 4^+, 364.1$		$1.9 \times 10^{36}$	$2.7 \times 10^{35}$	$8.9 \times 10^{33}$		$\geq 5.0 \times 10^{19}$ this work
$^{189}\text{Os}, 3/2^- \rightarrow ^{185}\text{W}, 3/2^-, \text{g.s.}$	1976.1(9)	$2.4 \times 10^{34}$	$4.8 \times 10^{29}$	$3.1 \times 10^{29}$		$\geq 3.5 \times 10^{15}$ this work
$^{189}\text{Os}, 3/2^- \rightarrow ^{185}\text{W}, 1/2^-, 23.5$		$1.8 \times 10^{35}$	$3.2 \times 10^{30}$	$1.1 \times 10^{32}$		$\geq 3.5 \times 10^{15}$ this work
$^{189}\text{Os}, 3/2^- \rightarrow ^{185}\text{W}, 5/2^-, 65.9$		$2.1 \times 10^{36}$	$3.1 \times 10^{31}$	$1.1 \times 10^{33}$		$\geq 7.6 \times 10^{17}$ this work
$^{190}\text{Os}, 0^+ \rightarrow ^{186}\text{W}, 0^+, \text{g.s.}$	1375.8(12)	$3.6 \times 10^{48}$	$2.0 \times 10^{47}$	$2.1 \times 10^{46}$		–
$^{190}\text{Os}, 0^+ \rightarrow ^{186}\text{W}, 2^+, 122.6$		$1.1 \times 10^{54}$	$4.9 \times 10^{52}$	$1.6 \times 10^{51}$		$\geq 1.2 \times 10^{19}$ this work
$^{190}\text{Os}, 0^+ \rightarrow ^{186}\text{W}, 4^+, 396.5$		$5.8 \times 10^{69}$	$1.1 \times 10^{68}$	$1.6 \times 10^{65}$		$\geq 8.6 \times 10^{19}$ this work
$^{192}\text{Os}, 0^+ \rightarrow ^{188}\text{W}, 0^+, \text{g.s.}$	361(4)	$1.7 \times 10^{153}$	$1.8 \times 10^{149}$	$1.4 \times 10^{140}$		$\geq 5.8 \times 10^{18}$ this work
$^{192}\text{Os}, 0^+ \rightarrow ^{188}\text{W}, 2^+, 143.2$		$1.6 \times 10^{215}$	$5.5 \times 10^{209}$	$9.9 \times 10^{190}$		$\geq 2.7 \times 10^{19}$ this work

developed or improved (see e.g. [2, 3, 4, 5, 6, 7, 8, 9, 10, 11] and references therein), in particular motivated by searches for stable or long-lived super-heavy isotopes [12, 13, 14] and predictions of their half-lives.

Improvements in the experimental sensitivity, especially related with the use of super-low-background set-ups located in underground laboratories, have led during the last decade to the discovery of  $\alpha$  decays which were not observed previously due to their extremely long half-lives. We refer the interested readers to [15] where the current status of the experimental searches for rare  $\alpha$  and  $\beta$  decays is reviewed. The half-life of  $^{174}\text{Hf}$  was remeasured recently (after publication of the review [15]) with improved accuracy as  $T_{1/2} = (7.0 \pm 1.2) \times 10^{16}$  yr with the help of a  $\text{Cs}_2\text{HfCl}_6$  scintillator [16].

All the seven naturally occurring osmium isotopes are potentially unstable relative to  $\alpha$  decay (see Table 1), however, only for two of them (with the highest  $Q_\alpha$  values) indications on their existence were obtained. For  $^{184}\text{Os}$ , only limits were known previously:  $T_{1/2} > 2.0 \times 10^{13}$  yr [17, 18] set with nuclear emulsions, and  $T_{1/2} > 5.6 \times 10^{13}$  yr [19] with proportional counter measurements of Os sample enriched in  $^{184}\text{Os}$  to 2.25%. However, recently an indication on  $\alpha$  decay of  $^{184}\text{Os}$  was found in geochemical measurements [20] where an excess of daughter  $^{180}\text{W}$  was measured in meteorites and terrestrial rocks; the half-life was determined as  $T_{1/2} = (1.1 \pm 0.2) \times 10^{13}$  yr, which is in contradictions with the results of the direct laboratory measurements. The decay of  $^{186}\text{Os}$  with  $T_{1/2} = (2.0 \pm 1.1) \times 10^{15}$  yr was observed in direct experiment with a semiconductor detector and an Os sample enriched in  $^{186}\text{Os}$  to 61.27% [21].

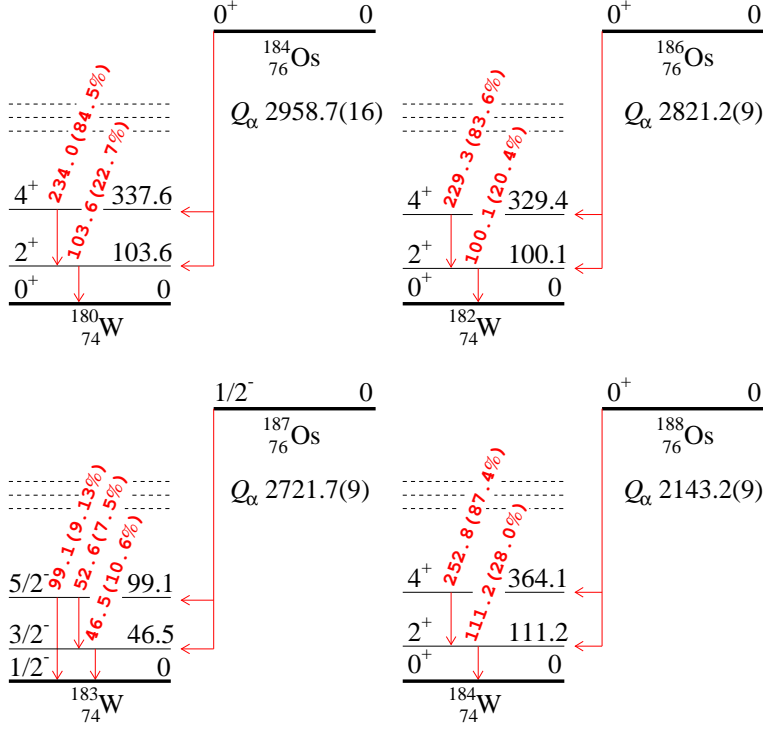


Figure 1: (Color online) Expected schemes of  $^{184}\text{Os}$ ,  $^{186}\text{Os}$ ,  $^{187}\text{Os}$  and  $^{188}\text{Os}$   $\alpha$  decay to the two first excited levels of daughter nuclei. The  $Q_\alpha$  values, energies of the levels and of the de-excitation  $\gamma$  quanta are given in keV; the probabilities of  $\gamma$  quanta emission are given in parentheses [28, 29, 30, 18].

The process of  $\alpha$  decay can be accompanied by the emission of  $\gamma$  quanta when the decay goes to excited level(s) of a daughter nucleus. In this work, we look for  $\gamma$  quanta expected in  $\alpha$  decays of the naturally occurring osmium nuclides to the two lowest excited levels of daughter nuclei (see Figs. 1 and 2 where expected schemes of  $\alpha$  decay of the osmium isotopes are shown). It should be noted that the  $^{189}\text{Os}$  and  $^{192}\text{Os}$  also  $\alpha$  decay to the ground state of the daughter nuclei can be searched for thanks to the  $\beta$ -instability of the daughter nuclides which is also accompanied by  $\gamma$  quanta. The experiment was realized with the help of ultra-low background HPGe  $\gamma$  spectrometry of a highly purified osmium metal sample with the natural isotopic composition. The isotopic composition of the osmium was measured precisely with the help of Negative Thermal Ionization Mass Spectrometry. The results of the previous stage of the experiment, which was devoted mainly to search for  $2\beta$  processes in  $^{184}\text{Os}$  and  $^{192}\text{Os}$ , were reported in [26, 27]. The main attention in the present study is focused on the search for  $\alpha$  decays with emission of  $\gamma$  quanta in  $^{184}\text{Os}$  and  $^{186}\text{Os}$ , taking into account the theoretically highest decay probabilities for these nuclides (see Table 1).

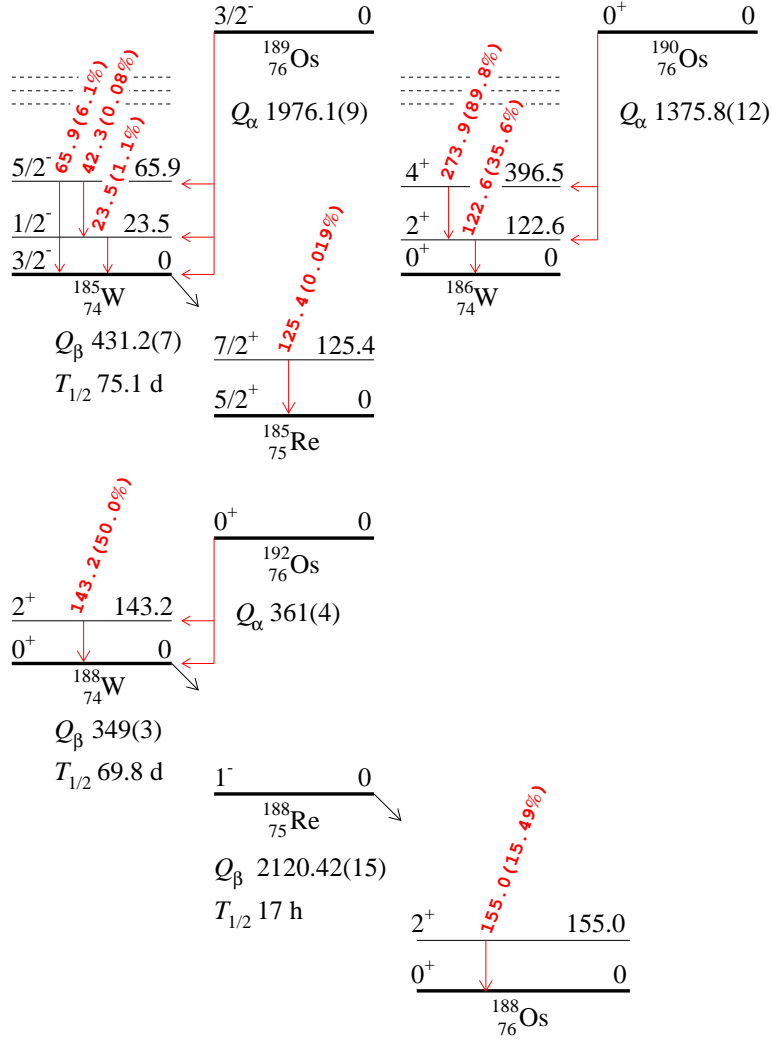


Figure 2: (Color online) Expected schemes of  $^{189}\text{Os}$  and  $^{190}\text{Os}$   $\alpha$  decay to the two first excited levels of daughter nuclei. The decay scheme of  $^{192}\text{Os}$  is also reported. The  $Q_\alpha$  values, energies of the levels and of the de-excitation  $\gamma$  quanta are given in keV; the probabilities of  $\gamma$  quanta emission are given in parentheses [31, 32, 33].

## 2 Experiment

### 2.1 Sample of osmium

Osmium in form of metal of at least 99.999% purity grade [34] was used in the present experiment. The material was obtained from osmium powder by electron-beam melting with further purification by electron-beam zone refining at the National Science Center “Kharkiv Institute of Physics and Technology” (Kharkiv, Ukraine). The osmium in form of four ingots with a total mass of 173 g was used in the first low-background experiment aiming at the search for double beta processes in  $^{184}\text{Os}$  and  $^{192}\text{Os}$  [26, 27]. Preliminary results of the searches for  $\alpha$  decay of  $^{184}\text{Os}$  and  $^{186}\text{Os}$  to the first excited levels of daughter nuclei were reported too [27].

The density of osmium metal is very high (in fact, osmium is the densest naturally occurring element: the sample density was estimated to be  $23\text{ g/cm}^3$ , while the reference value is  $22.587\text{ g/cm}^3$  [35]). Thus,  $\gamma$ -ray quanta expected to be emitted in the  $\alpha$  decays of the naturally occurring osmium isotopes are strongly absorbed in the sample. To increase the detection efficiency the ingots were cut into thin slices with a thickness of  $(0.79 - 1.25)$  mm by using a method of electroerosion cutting with brass wire in kerosene. The slices were then etched in a solution of nitric and hydrochloric acids and washed by ultra-pure water.

### 2.2 Precise measurements of the osmium isotopic composition

The Os isotopic composition was analysed in the John de Laeter Centre at Curtin University (Perth, Western Australia). In order to achieve a complete digestion of the pure Os metal, the Carius tube digestion method modified from Shirey and Walker [36] was applied. Approximately 0.5 mg of Os metal was consumed for each of the two samples studied. The acid digestion was done using concentrated acids (3 mL of purged double-distilled  $\text{HNO}_3$  and 1 mL of triple-distilled  $\text{HCl}$ ). This mixture was chilled and sealed in previously cleaned Pyrex<sup>TM</sup> borosilicate Carius Tubes and heated up to  $220\text{ }^\circ\text{C}$  for 60 h. Osmium was extracted from the acid solution by chloroform solvent extraction [37], then back-extracted into  $\text{HBr}$ , followed by purification via microdistillation [38]. The purified Os fraction of each of the two samples was loaded onto five separate Pt filaments (ten in total), and measured using Negative Thermal Ionisation Mass Spectrometry (N-TIMS) on a Thermo-Fisher Triton<sup>TM</sup> mass spectrometer using Faraday cup collectors. The beam for samples studied was maintained at  $\sim 10^{-11}\text{ A}$  (for  $^{192}\text{Os}$ ) for extended period of time for Os metal (100 blocks of 10 cycles were collected), allowing to obtain a standard error of the mean precision below 10 ppm level [39]. The measured oxide ion ratios  $\text{OsO}_3^-$  were corrected for isobaric oxygen interferences to obtain element ratios, which were corrected for mass fractionation using a  $^{192}\text{Os}/^{188}\text{Os}$  value of 3.08271 [40].

The pure Os metal gave the average of  $^{187}\text{Os}/^{188}\text{Os}$  ratio  $0.14179 \pm 0.00009$  at 95% C.L. To monitor the intermediate precision over a period of 12 months of the N-TIMS instrument for Os, an AB-2 Os reference solution (University of Alberta) was measured as part of the protocol. The AB-2 Os standard yielded the  $^{187}\text{Os}/^{188}\text{Os}$  ratio  $0.10687 \pm 0.00012$  (95% C.L.) during the 12 month period of the measurements, which is consistent with that reported by Selby and Creaser [41] ( $0.10684 \pm 0.00004$ ). The total procedural blank for Os was 0.50 pg, its contribution is insignificant for the sample studied. The  $^{187}\text{Os}/^{188}\text{Os}$  ratio for the blank was  $0.201 \pm 0.020$  ( $n = 2$ ).

A summary of the osmium isotopic composition, as well as numbers of nuclei of the osmium

Table 2: Isotopic composition ( $\delta$ ) of the osmium measured in the present work and the numbers of nuclei of each isotope in the sample calculated by using the measured isotopic concentrations. The representative isotopic abundances from [43] are given too.

Isotope	$\delta$ (%)		Number of nuclei in the sample
	IUPAC [43]	this work	
$^{184}\text{Os}$	0.02(2)	0.0170(7)	$6.35(26) \times 10^{19}$
$^{186}\text{Os}$	1.59(64)	1.5908(6)	$5.9405(25) \times 10^{21}$
$^{187}\text{Os}$	1.96(17)	1.8794(6)	$7.0182(25) \times 10^{21}$
$^{188}\text{Os}$	13.24(27)	13.253(3)	$4.9490(14) \times 10^{22}$
$^{189}\text{Os}$	16.15(23)	16.152(4)	$6.0316(18) \times 10^{22}$
$^{190}\text{Os}$	26.26(20)	26.250(8)	$9.8025(34) \times 10^{22}$
$^{192}\text{Os}$	40.78(32)	40.86(5)	$1.5258(19) \times 10^{23}$

isotopes in the sample are given in Table 2. The accuracy of the  $^{184}\text{Os}$  measurement [0.0170(7)%] is similar to the accuracy of the “best measurement from a single terrestrial source” [0.0197(5)%] [42], and is definitely higher than the error scale recommended by IUPAC: 0.02(2)% [43]. The  $^{186}\text{Os}$  isotopic concentration was measured with a much higher accuracy than the recommended representative isotopic abundance too. Also for other Os isotopes the errors in the present study are much smaller than the ones given in [43]<sup>2</sup>.

### 2.3 Low-background measurements

The Os slices (see Sec. 2.1) with a total mass of 117.96(2) g were fixed on the inner surface of a plastic Petri dish (with a thickness of 0.8 mm) with the help of Scotch 811 removable tape. The Petri dish with the Os slices was installed directly on the aluminium end-cap of the cryostat of the ultra-low background Broad-Energy Germanium (BEGe) detector with a volume of 112.5 cm<sup>3</sup> (Fig. 2.3). The detector, thanks to a very thin dead layer of 0.4  $\mu\text{m}$ , offers a high sensitivity to low-energy photons. The detector with the Os sample was shielded by layers of  $\approx 5$  cm thick copper and 20 cm thick lead.

The low-background measurements were carried out at the STELLA (SubTerranean Low Level Assay) facility of the Gran Sasso National Laboratory of the INFN (Italy) [45]. The laboratory is located at a depth of  $\approx 3600$  meters of water equivalent. The data were taken in 10 runs with a total measurement time of 15851 h. The energy scale of the detector was measured with  $\gamma$  sources in the beginning of the experiment. Then the data of each run were re-calibrated by using clear and intensive background  $\gamma$  peaks of  $^{40}\text{K}$ ,  $^{208}\text{Tl}$ ,  $^{210}\text{Pb}$ ,  $^{214}\text{Pb}$  and  $^{214}\text{Bi}$  to improve the energy resolution in the final sum spectrum. The dependence of energy

<sup>2</sup>Moreover, there is still a room for improvement of the Os isotopic composition accuracy as it was recently demonstrated in [44].



Figure 3: (Color online) Left photograph: the main part of the osmium slices before assembling on a plastic Petri dish (the scale is in centimeters). Right photograph: arrangement of the sample on a cryostat end-cap (unshielded detector, not the same used in the measurements).

resolution (full width at half maximum, FWHM) on energy of  $\gamma$ -ray quanta ( $E_\gamma$ , in keV) in the sum energy spectrum can be approximated by the following function:

$$\text{FWHM (keV)} = 0.57(5) + 0.029(2) \times \sqrt{E_\gamma}. \quad (1)$$

The re-calibration procedure allowed to improve the detector energy resolution in the final spectrum by 13% (at energy 100 keV) in comparison to the sum energy spectrum obtained without the correction.

## 3 Results and discussion

### 3.1 Radioactive contamination of the osmium sample

The energy spectrum measured with the Os sample for 15851 h is shown in Fig. 4 together with the background energy spectrum taken over 1660 h. One can see that the counting rate in the spectrum measured with the Os sample below  $\approx 0.4$  MeV is lower than in the background data. The difference is due to the very high density of osmium. As a result, the Os sample is effectively absorbing radiations from the shielding materials around the detector (mainly bremsstrahlung  $\gamma$ -ray from  $^{210}\text{Pb}$  in the lead details of the shielding), and thus reducing the count rate at low energies.

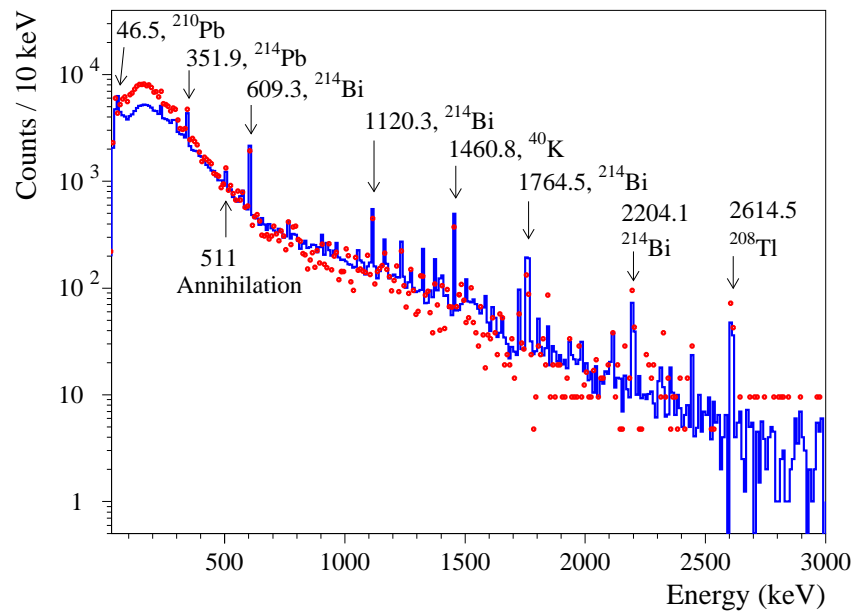


Figure 4: Energy spectra accumulated for 15851 h with the Os sample (solid line, blue online) and background energy spectrum measured over 1660 h without sample (dots; red online). The background data are normalized to the time of measurements with the Os sample. Energies of  $\gamma$ -ray peaks are in keV.



The peaks in the energy spectra belong mainly to  $\gamma$ -ray quanta of naturally occurring primordial radionuclides:  $^{40}\text{K}$ , and daughters of  $^{232}\text{Th}$ ,  $^{235}\text{U}$ ,  $^{238}\text{U}$ . There are also weak peaks in both the spectra that can be ascribed to  $^{60}\text{Co}$  and  $^{137}\text{Cs}$ . Specific activities of the radionuclides in the Os sample were calculated with the following formula:

$$A = (S_{\text{sample}}/t_{\text{sample}} - S_{\text{bg}}/t_{\text{bg}})/(\eta \cdot \varepsilon \cdot m), \quad (2)$$

where  $S_{\text{sample}}$  ( $S_{\text{bg}}$ ) is the area of a peak in the sample (background) spectrum;  $t_{\text{sample}}$  ( $t_{\text{bg}}$ ) is the time of the sample (background) measurement;  $\eta$  is the  $\gamma$ -ray emission intensity;  $\varepsilon$  is the full energy peak efficiency;  $m$  is the sample mass. The detection efficiencies to  $\gamma$ -ray quanta were calculated using the GEANT4 simulation package [46, 47, 48], the decay events were generated homogeneously in the Os sample. If no statistically significant peak excess was observed (the cases of  $^{60}\text{Co}$ , daughters of  $^{232}\text{Th}$ ,  $^{235}\text{U}$  and  $^{238}\text{U}$ ), only upper limits on the specific activities of the radioactive impurities in the sample were set. A summary of the Os sample radioactive contamination is given in Table 3.

Table 3: Radioactive contamination of the Os sample measured by the ultra-low-background BEGe  $\gamma$  detector.

Decay chain	Radionuclide	Specific activity (mBq/kg)
	$^{40}\text{K}$	$11 \pm 4$
	$^{60}\text{Co}$	$\leq 1.3$
	$^{137}\text{Cs}$	$0.5 \pm 0.1$
$^{232}\text{Th}$	$^{228}\text{Ra}$	$\leq 6.6$
	$^{228}\text{Th}$	$\leq 16$
$^{235}\text{U}$	$^{235}\text{U}$	$\leq 8.0$
	$^{231}\text{Pa}$	$\leq 3.5$
	$^{227}\text{Ac}$	$\leq 1.1$
$^{238}\text{U}$	$^{238}\text{U}$	$\leq 35$
	$^{226}\text{Ra}$	$\leq 4.4$
	$^{210}\text{Pb}$	$\leq 180$

### 3.2 Limits on $\alpha$ decays of $^{184}\text{Os}$ and $^{186}\text{Os}$ to the first excited levels of daughter nuclei

There are no peaks in the energy spectrum measured with the Os sample that can be interpreted as  $\alpha$  decay of naturally occurring osmium nuclides. Thus, by analysis of the data one can set half-life limits on the processes searched for with the help of the following formula:

$$\lim T_{1/2} = \frac{N \cdot \ln 2 \cdot \eta \cdot \varepsilon \cdot t}{\lim S}, \quad (3)$$

where  $N$  is the number of nuclei of the isotope of interest (given in Table 2),  $\eta$  is the  $\gamma$  quanta emission intensity (see Figs. 1 and 2),  $\varepsilon$  is the detection efficiency for  $\gamma$  quanta expected in the decays,  $t$  is the time of measurement (15851 h), and  $\lim S$  is the upper limit on the number of events of the effect searched for which can be excluded at a given C.L.

The detection efficiencies to  $\gamma$ -ray quanta expected in the decays searched for were Monte Carlo simulated with the GEANT4 [46, 47, 48] and the EGSnrc [49] packages in two geometries: with uniform and granulated source. In the “uniform geometry” the source was approximated by a disc of 88 mm in diameter with a thickness of 0.88 mm, plus a ring with an inner diameter of 90 mm and a height of 8 mm, with the same thickness. The “granulated geometry” reproduces the actual geometry of the source in a more accurate way (separate objects with gaps between them). Both the GEANT4 and EGSnrc codes give compatible results with the standard deviation of the relative difference 2.7% for  $\gamma$  quanta in the energy range from 46.5 keV to 273.0 keV (for the “uniform geometry”). The main difference in the simulations results is due to the different source geometries. The relative difference between the detection efficiencies for the “uniform” and “granulated” geometries decreases from 11.9% to 4.5% with increase of  $\gamma$  quanta energy from 46.5 keV to 273.0 keV, with a systematically higher efficiency for the granulated source. The higher efficiency for the “granulated geometry” can be explained by the contribution of  $\gamma$ -quanta events emitted from the side parts of the osmium slices (in contrary to the uniform source geometry with no gaps in the Os material). The increase of the difference with decrease of the  $\gamma$ -quanta energy can be explained by the “edge effect” that is more significant at low energies. Taking into account that the “granulated geometry” describes the sample in a more accurate way we use the detection efficiencies obtained with this geometry for the further analysis. The full energy peak detection efficiencies for the  $\alpha$  decays under study are presented in Table 4.

Table 4: Full energy peak detection efficiencies,  $\varepsilon$ , for signature  $\gamma$ -ray quanta with energy  $E_\gamma$ ,  $\gamma$  quanta emission intensity  $\eta$ , measured numbers of events ( $S$ ), their standard deviations ( $\Delta S$ ) and estimated values of  $\lim S$  (see discussions in the text) for  $\alpha$  transitions with emission of  $\gamma$  quanta in naturally occurring osmium isotopes. The relative systematic uncertainties  $\sigma_r$  and factors  $a$  (see text below) to take into account the systematic uncertainties are given in the last two columns.

Transition	$E_\gamma$ (keV)	$\eta$	$\varepsilon$	$S$	$\Delta S$	$\lim S$	$\sigma_r$	$a$
$^{184}\text{Os}, 0^+ \rightarrow ^{180}\text{W}, 2^+, 103.6$	103.6	0.227	0.01382	-7.3	21.3	28.1	0.130	1.301
$^{184}\text{Os}, 0^+ \rightarrow ^{180}\text{W}, 4^+, 337.6$	234.0	0.845	0.05097	22.4	24.6	62.7	0.095	1.183
$^{186}\text{Os}, 0^+ \rightarrow ^{182}\text{W}, 2^+, 100.1$	100.1	0.204	0.01274	8.6	21.8	44.4	0.135	1.325
$^{186}\text{Os}, 0^+ \rightarrow ^{182}\text{W}, 4^+, 329.4$	229.3	0.836	0.05090	-14.2	24.9	28.0	0.206	1.893
$^{187}\text{Os}, 1/2^- \rightarrow ^{183}\text{W}, 3/2^-, 46.5$	46.5	0.106	0.00695	1272	42	1341	0.120	1.493
$^{187}\text{Os}, 1/2^- \rightarrow ^{183}\text{W}, 5/2^-, 99.1$	99.1	0.0913	0.01219	2.9	22.8	40.3	0.117	1.254
$^{188}\text{Os}, 0^+ \rightarrow ^{184}\text{W}, 2^+, 111.2$	111.2	0.280	0.01629	3.8	30.7	54.1	0.150	1.568
$^{188}\text{Os}, 0^+ \rightarrow ^{184}\text{W}, 4^+, 364.1$	252.8	0.874	0.05200	-2.9	25.8	39.7	0.140	1.420
$^{189}\text{Os}, 3/2^- \rightarrow ^{185}\text{W}, 3/2^-, \text{g.s.}$	125.4	0.00019	0.02098	-2.7	24.9	38.4	0.245	2.233
$^{189}\text{Os}, 3/2^- \rightarrow ^{185}\text{W}, 5/2^-, 65.9$	65.9	0.061	0.01936	30.7	23.6	69.4	0.189	1.689
$^{190}\text{Os}, 0^+ \rightarrow ^{186}\text{W}, 2^+, 122.6$	122.6	0.356	0.02085	17.3	24.4	57.3	0.122	1.296
$^{190}\text{Os}, 0^+ \rightarrow ^{186}\text{W}, 4^+, 396.5$	273.9	0.898	0.05197	21.3	24.3	61.2	0.067	1.090
$^{192}\text{Os}, 0^+ \rightarrow ^{188}\text{W}, 0^+, \text{g.s.}$	155.0	0.1549	0.03220	93.7	29.3	142	0.081	1.159
$^{192}\text{Os}, 0^+ \rightarrow ^{188}\text{W}, 2^+, 143.2$	143.2	0.500	0.02898	42.5	27.0	86.8	0.090	1.180

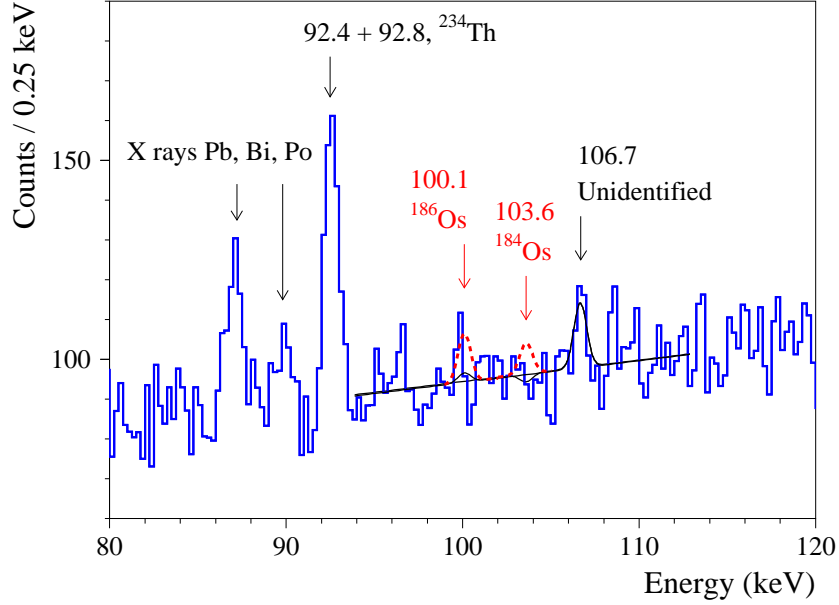


Figure 5: Energy spectrum measured with the Os sample for 15851 h in the region where the peaks with energies 100.1 keV and 103.6 keV after the  $\alpha$  decay of the  $^{186}\text{Os}$  and of the  $^{184}\text{Os}$  to the first excited levels of daughter nuclei are expected. The fits of the data by the background model (see text) are shown by solid lines (the fits for the 100.1 keV and 103.6 keV peaks are almost indistinguishable). The peaks with energies 100.1 keV and 103.6 keV excluded at 90% C.L. are shown by dashed lines.

To estimate the values of  $\lim S$ , the energy spectrum taken with the Os sample was fitted in the region of interest for a certain transition with the models accounting for the effect searched for and for the background. For instance, to estimate value of  $\lim S$  for the decay of the  $^{184}\text{Os}$  to the first excited level of  $^{180}\text{W}$ , the energy spectrum was fitted by a background model constructed from a linear function (to describe the continuous distribution), a peak with the energy of 103.6 keV (the effect searched for), and an unidentified peak with energy  $\approx 107$  keV. The data were fitted by the model with 5 free parameters: two parameters of the linear function, an area of the 103.6 keV peak, an area and a position of the unidentified peak. The peaks widths were fixed according to the estimated energy dependence of the detector energy resolution (see formula given in eq. (1)). The best fit was achieved in the energy interval (93.75 – 112.75) keV with  $\chi^2 = 33.9$  for 72 degrees of freedom. The Fig. 5 shows the energy spectrum measured with the Os sample in the region of interest and its fit by the above described model. A similar analysis was performed also for the 100.1 keV peak expected in the  $\alpha$  decay of  $^{186}\text{Os}$  to the first excited level of  $^{182}\text{W}$ .

The fits return the 100.1 keV and 103.6 keV peaks areas ( $8.6 \pm 21.8$ ) counts and ( $-7.3 \pm 21.3$ ) counts, respectively, that is no evidence of the effects searched for<sup>3</sup>. By using the recommendations [50] we get the following upper limits on the peaks areas:  $\lim S = 44.4$  counts (for the 100.1 keV peak), and  $\lim S = 28.1$  counts (103.6 keV) at 90% C.L. (the excluded peaks are shown in Fig. 5), that correspond to the lower half-life limits  $T_{1/2}(^{184}\text{Os}) > 8.9 \times 10^{15}$  yr and  $T_{1/2}(^{186}\text{Os}) > 4.4 \times 10^{17}$  yr, respectively. However, the limits include only statistical errors.

<sup>3</sup>The area of the unidentified peak is ( $60 \pm 23$ ) counts, the energy of the peak is ( $106.67 \pm 0.15$ ) keV.

Possible sources of systematic uncertainties of the half-life limits are listed in Table 5. The systematic uncertainties of the detection efficiencies were conservatively estimated as the relative differences between the GEANT4 simulations results with the “granulated” and “uniform” geometries. Variations of  $\lim S$  depending on the fit interval were estimated by analysis of  $\lim S$  distributions obtained from the fit of the data in the energy intervals within (93.5 – 96) keV for the starting point, and (110 – 116) keV for the final point, with a step of 0.25 keV. An impact of the isotopic abundance measurements uncertainties (presented in Table 2) was taken in consideration too. The total relative systematic errors  $\sigma_r$  were obtained by adding all the systematic contributions in quadrature.

Table 5: Estimated relative systematic uncertainties of the  $^{184}\text{Os}$  and  $^{186}\text{Os}$  half-life limits relative to  $\alpha$  decays to the first excited levels of the daughter nuclei.

Source	Nuclide	
	$^{184}\text{Os}$	$^{186}\text{Os}$
Detection efficiency	0.098	0.118
Interval of fit	0.076	0.065
Isotopic abundance	0.041	0.0004
Total relative systematic error ( $\sigma_r$ )	0.131	0.135

The systematic uncertainties  $\sigma_r$  can be introduced into the obtained lower half-life limits by correction of the upper limits on the number of excluded events:

$$\lim S' = \lim S \times a, \quad (4)$$

where  $\lim S'$  is a corrected upper limit, and the factor  $a$  is expressed by the formula proposed in [51]:

$$a = [1 + (\lim S - S) \times \sigma_r^2 / 2]. \quad (5)$$

After the correction the following half-life limits of  $^{184}\text{Os}$  and  $^{186}\text{Os}$  relative to  $\alpha$  decay to the first excited levels of the daughter nuclei were obtained:

$$T_{1/2}(^{184}\text{Os}) > 6.8 \times 10^{15} \text{ yr},$$

$$T_{1/2}(^{186}\text{Os}) > 3.3 \times 10^{17} \text{ yr}.$$

It should be noted that the limits substantially exceed the present theoretical predictions (see Table 1). In particular, the limits are one order of magnitude higher than the estimates obtained by using the empirical relationships based on the unified model for  $\alpha$  decay and  $\alpha$  capture (UMADAC) [5] and the half-life values calculated in the framework of a semi-empirical model based on the quantum mechanical tunneling mechanism through a potential barrier [11].

### 3.3 Limits on other $\alpha$ decays of osmium nuclides with emission of $\gamma$ quanta

Due to the smaller energy release, the theoretical predictions on half-lives of  $\alpha$  decays of  $^{184}\text{Os}$  and  $^{186}\text{Os}$  to the second excited levels of daughter nuclei, not to say for  $\alpha$  decays of other

osmium nuclides, are much longer. Thus, the sensitivity of the present experiment looks too low to detect the processes. Nevertheless, the experimental data were used to analyze other possible decays of the osmium nuclides too.

Examples of the energy spectrum fits in the regions of interest for the  $\alpha$  decays of  $^{184}\text{Os}$  and  $^{186}\text{Os}$  to the second excited levels of  $^{180}\text{W}$  and  $^{182}\text{W}$ , and for the  $\alpha$  decays of  $^{187}\text{Os}$  to the first 46.5 keV excited level of  $^{183}\text{W}$  are shown in Fig. 6. Unfortunately, the signature  $\gamma$  peak expected in the decay of  $^{187}\text{Os}$  interferences strongly with the 46.5 keV  $\gamma$ -ray peak of  $^{210}\text{Pb}$  (daughter of  $^{222}\text{Rn}$  from the  $^{238}\text{U}$  family), typically present in low-background  $\gamma$  spectra. Thus, we accept the peak area (1272 counts) plus its standard error (42 counts) multiplied by 1.64 to get an estimation of  $\text{lim } S$  for this decay channel at 90% C.L.

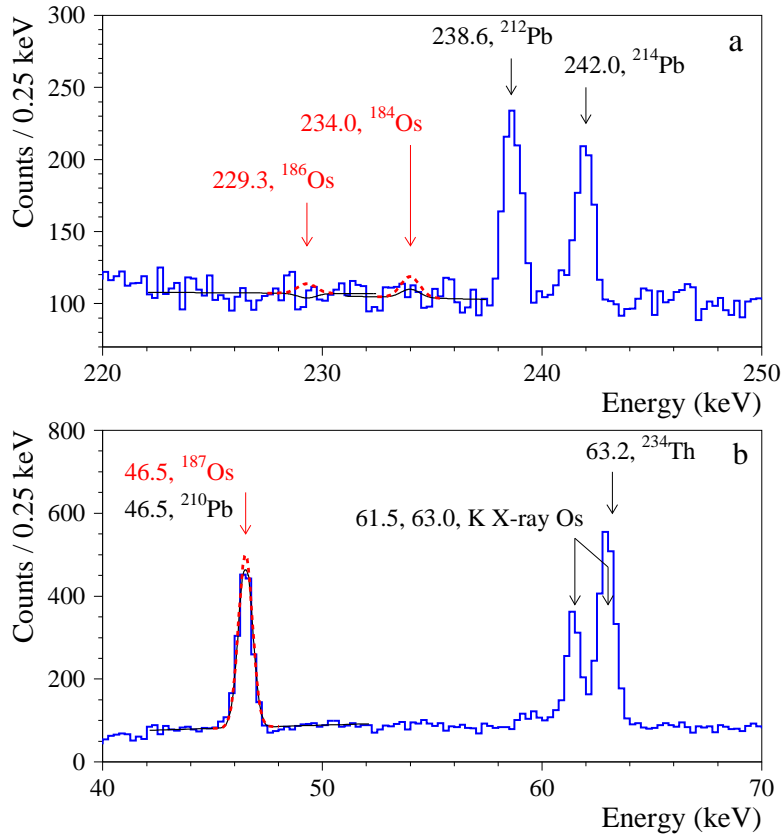


Figure 6: Energy spectrum measured with the Os sample for 15851 h in the region where peaks with energies 234.0 keV ( $\alpha$  decay of  $^{184}\text{Os}$  to the 337.6 keV excited level of  $^{180}\text{W}$ ) and 229.3 keV ( $\alpha$  decay of  $^{186}\text{Os}$  to the 329.4 keV excited level of  $^{182}\text{W}$ ) are expected (a). Low energy part of the spectrum, where a peak with an energy of 46.5 keV is expected ( $\alpha$  decay of  $^{187}\text{Os}$  to the 46.5 keV excited level of  $^{183}\text{W}$ ) (b). The existing peak with this energy can be explained by  $\gamma$  quanta after  $\beta$  decay of  $^{210}\text{Pb}$ . Fits of the data by the background model are shown by solid lines. The peaks searched for, excluded at 90% C.L., are shown by dashed lines.

To estimate the  $\text{lim } S$  values for other possible decay channels the experimental spectrum was analyzed in the different energy intervals in a similar way as described above. The detection efficiencies and the emission intensities for the signature  $\gamma$ -ray quanta, the obtained values of  $S$ ,  $\Delta S$  and  $\text{lim } S$ , the relative systematic errors  $\sigma_r$  and the factors  $a$  to account systematic uncertainties of the limits are given in Table 4, while the half-life limits on the  $\alpha$  decays of

naturally occurring osmium isotopes with emission of  $\gamma$  quanta are summarized in Table 1.

It should be noted that for  $^{189}\text{Os}$  and  $^{192}\text{Os}$  also decays to the ground states of the daughter nuclei (in general, to any states of the daughter nuclei) were set due to the  $\beta$ -instability of the daughter nuclides with lifetimes short enough to be in equilibrium with the parent nuclides. However, the theoretically estimated half-lives of the nuclides are very long to be observed in a realistic experiment. At the same time our experiment is not sensitive to the  $\alpha$  decay of  $^{189}\text{Os}$  to the first 23.5 keV excited level of  $^{185}\text{W}$  due to an approximately two times higher energy threshold of the detector  $\approx 42$  keV. Nevertheless, the limit obtained for the g.s. to g.s. transition (by using the  $\beta$ -instability of  $^{185}\text{W}$ ) is valid for  $\alpha$  decay to all levels, including excited ones (it should be stressed, however, that also this decay is expected to be too rare to be observed).

It should be also noted that a significant area ( $93.7 \pm 29.3$ ) counts of the 155.0 keV peak (expected in the decay sequence  $^{192}\text{Os} \rightarrow ^{188}\text{W} \rightarrow ^{188}\text{Re} \rightarrow ^{188}\text{Os}$ ) was interpreted as absence of the effect searched for. The peak can be explained by several sources:

- $\gamma$ -ray quanta with energy 154.0 keV of  $^{228}\text{Ac}$  (daughter of  $^{228}\text{Ra}$  from the  $^{232}\text{Th}$  family; emission probability 0.722%).
- $\gamma$ -ray quanta with energy 154.2 keV of  $^{223}\text{Ra}$  (daughter of  $^{227}\text{Ac}$  from the  $^{235}\text{U}$  family; emission probability 5.7%).
- $\gamma$ -ray quanta with energy 155.0 keV of  $^{188}\text{Re}$  (daughter of  $^{188}\text{W}$  that can be cosmogenically-produced in osmium; emission probability 15.49%).
- Thermal neutron capture  $\gamma$ -ray quanta with energy 155.0 keV emitted with an intensity 65% after neutron-captures in  $^{187}\text{Os}$  that has a rather big thermal neutron cross section ( $320 \pm 10$  barn).

Precise determination of the 155.0 keV peak area is difficult since the thermal neutrons flux in the set-up, activity and localization of the  $^{228}\text{Ra}$  and  $^{227}\text{Ac}$  are unknown. Also estimation of cosmogenic  $^{188}\text{W}$  activity in the Os sample is not a trivial task. Here we conservatively ascribe all the counts in the 155 keV peak (with error bar) to the  $^{192}\text{Os}$  alpha decay.

## 4 Theoretical estimates of the half-lives

We calculated theoretical half-lives of Os nuclides relative to  $\alpha$  decay using the semi-empirical formulae [23] based on the liquid drop model and the description of  $\alpha$  decay as a very asymmetric fission process. As well, the cluster model of Refs. [24, 25] was used. The approaches [23, 24, 25] were tested with a set of experimental half-lives of almost four hundred  $\alpha$  emitters and demonstrated good agreement between calculated and experimental  $T_{1/2}$  values, mainly inside a factor of 2–3. For Os  $\alpha$  decays with a difference between spins and parities of the parent and the daughter nuclei, which resulted in non-zero angular momentum  $l$  of the emitted  $\alpha$  particle, we take into account the additional hindrance factor  $HF$ , calculated in accordance with [52] (for the lowest possible  $l$  value). In particular, for the most important  $\alpha$  decays of  $^{184}\text{Os}$  and  $^{186}\text{Os}$  to the first excited levels of the daughter nuclei ( $0^+ \rightarrow 2^+$  transitions),  $HF \simeq 2.0$ .

The approaches [23, 24, 25] demonstrated reliable predictions in our previous experiments where some very rare  $\alpha$  decays were observed at the first time:

- for  $^{180}\text{W}$ , the calculated values are<sup>4</sup>  $T_{1/2} = 2.1 \times 10^{18}$  yr [23] and  $T_{1/2} = 8.5 \times 10^{17}$  yr [24, 25] while the experimental values are in the range of  $(1.0 - 1.8) \times 10^{18}$  yr [53, 54, 55, 56, 57];
- for  $^{151}\text{Eu}$ , the calculated values are  $T_{1/2} = 3.6 \times 10^{18}$  yr [23] and  $T_{1/2} = 2.9 \times 10^{17}$  yr [24, 25] with the experimental half-life near  $5 \times 10^{18}$  yr [58, 59];
- for  $\alpha$  decay of  $^{190}\text{Pt}$  to the first excited level of  $^{186}\text{Os}$  ( $E_{exc} = 137.2$  keV), the calculated values are  $T_{1/2} = 4.5 \times 10^{13}$  yr [23] and  $T_{1/2} = 2.1 \times 10^{13}$  yr [24, 25] while the experimental value is  $(2.2 \pm 0.6) \times 10^{14}$  yr [60]<sup>5</sup>;
- it is interesting to note that for  $^{174}\text{Hf}$  the calculated values  $T_{1/2} = 7.4 \times 10^{16}$  yr [23] and  $T_{1/2} = 3.5 \times 10^{16}$  yr [24, 25] were in strong contradiction with the old experimental value of  $(2.0 \pm 0.4) \times 10^{15}$  yr [61] (by factor of 17 – 38). However, recent measurements gave new experimental value of  $(7.0 \pm 1.2) \times 10^{16}$  yr [16] in a good agreement with calculations [23, 24, 25].

The  $T_{1/2}$  values calculated in accordance with [23, 24, 25] are presented in Table 1. In addition, we give the results obtained here with the semi-empirical formulae of Ref. [5] which also were successfully tested with about four hundred experimental  $\alpha$  decays and which take into account non-zero  $l$  explicitly. Also, recent calculations of Ref. [11] for Os isotopes, including transitions to the excited daughter levels, are presented in Table 1.

## 5 Conclusions

A search for the alpha activity accompanied by the emission of  $\gamma$ -ray quanta in naturally occurring osmium isotopes was realized by an ultra-low background Broad-Energy Germanium  $\gamma$  detector located deep underground at the Gran Sasso National Laboratory of INFN (Italy). A sample of ultra-pure osmium with a mass of 118 g, composed of thin osmium slices with an average thickness of 0.88 mm, was used as a source of the decays. The isotopic composition of osmium in the sample was precisely measured with the help of Negative Thermal Ionisation Mass Spectrometry, that is especially important for the isotope  $^{184}\text{Os}$  (theoretically the shortest living candidate) whose representative isotopic abundance was given with a very big uncertainty of  $\pm 100\%$  [43].

No  $\gamma$ -ray quanta expected in the decays searched for were observed but lower limits on the processes were set at level of  $\lim T_{1/2} \sim 10^{15} - 10^{19}$  yr. The half-life limits for  $\alpha$  decays of  $^{184}\text{Os}$  and  $^{186}\text{Os}$  to the first excited levels of daughter nuclei have been set at 90% C.L. as  $T_{1/2} \geq 6.8 \times 10^{15}$  yr and  $T_{1/2} \geq 3.3 \times 10^{17}$  yr, respectively. The limits exceed substantially the present theoretical estimations of the decays probabilities that are within  $T_{1/2} \sim (0.6 - 3) \times 10^{15}$  yr for  $^{184}\text{Os}$  and  $T_{1/2} \sim (0.3 - 2) \times 10^{17}$  yr for  $^{186}\text{Os}$ .

A new stage of the experiment is in progress by using an advanced geometry with the osmium sample placed directly on the BEGe detector inside its cryostat to increase the detection efficiency to the low energy  $\gamma$ -ray quanta expected in the theoretically fastest decays of  $^{184}\text{Os}$  and  $^{186}\text{Os}$  to the first excited levels of the daughter nuclei. Obviously, a further improvement of the experimental sensitivity to the decays with the highest decay probabilities can be achieved by using samples of osmium enriched in the  $^{184}\text{Os}$ ,  $^{186}\text{Os}$  and  $^{187}\text{Os}$  isotopes. Observation of other Os isotopes  $\alpha$ -instability looks practically problematic taking into account the very long theoretically predicted half-lives.

<sup>4</sup>We use here for calculations the AME2016  $Q_\alpha$  values from [22].

<sup>5</sup>We corrected here the original value of  $T_{1/2} = 2.6 \times 10^{14}$  yr [60] calculated for  $^{190}\text{Pt}$  natural abundance of  $\delta = 0.014\%$  with the last IUPAC recommended value of  $\delta = 0.012\%$  [43].

## 6 Acknowledgments

D.V.K. and O.G.P. were supported in part by the project “Investigation of double beta decay, rare alpha and beta decays” of the program of the National Academy of Sciences of Ukraine “Laboratory of young scientists” (the grant number 0120U101838).

## References

- [1] E. Rutherford, Uranium radiation and the electrical conduction produced by it, *Philos. Mag. (Ser. 5)* 47 (1899) 109.
- [2] V.Yu. Denisov, A.A. Khudenko,  $\alpha$ -Decay half-lives,  $\alpha$ -capture, and  $\alpha$ -nucleus potential, *At. Data Nucl. Data Tables* 95 (2009) 815; erratum *ibid.* 97 (2011) 187.
- [3] D.N. Poenaru, R.A. Gherghescu, W. Greiner, Simple relationships for  $\alpha$ -decay half-lives, *J. Phys. G* 39 (2012) 015105.
- [4] Y. Qian, Z. Ren, Half-lives of  $\alpha$  decay from natural nuclides and from superheavy elements, *Phys. Lett. B* 738 (2014) 87.
- [5] V.Yu. Denisov, O.I. Davidovskaya, I.Yu. Sedykh, Improved parametrization of the unified model for  $\alpha$  decay and  $\alpha$  capture, *Phys. Rev. C* 92 (2015) 014602.
- [6] K.P. Santhosh, I. Sukumaran, B. Priyanka, Theoretical studies on the alpha decay of  $^{178-220}\text{Pb}$  isotopes, *Nucl. Phys. A* 935 (2015) 28.
- [7] N. Ashok, D.M. Joseph, A. Joseph, Cluster decay in osmium isotopes using Hartree-Fock-Bogoliubov theory, *Mod. Phys. Lett. A* 31 (2016) 1650045.
- [8] B. Sahu, S. Bhoi, Viola-Seaborg relation for  $\alpha$ -decay half-lives: Update and microscopic determination of parameters, *Phys. Rev. C* 93 (2016) 044301.
- [9] S. Zhang et al., Improved semi-empirical relationship for  $\alpha$ -decay half-lives, *Phys. Rev. C* 95 (2017) 014311.
- [10] D.T. Akrawy, D.N. Poenaru, Alpha decay calculations with a new formula, *J. Phys. G* 44 (2017) 105105.
- [11] O.A.P. Tavares, M.L. Terranova, Partial alpha-decay half-lives for alpha-emitting Osmium isotopes: Accurate determinations by a semi-empirical model, *Appl. Rad. Isot.* 160 (2020) 109034.
- [12] S. Hofmann, Super-heavy nuclei, *J. Phys. G* 42 (2015) 114001.
- [13] Yu.Ts. Oganessian, A. Sobiczewski, G.M. Ter-Akopian, Superheavy nuclei: from predictions to discovery, *Phys. Scripta* 92 (2017) 023003.
- [14] S.A. Giuliani et al., Superheavy elements: Oganesson and beyond, *Rev. Mod. Phys.* 91 (2019) 011001.



- [15] P. Belli et al., Experimental searches for rare alpha and beta decays, *Eur. Phys. J. A* 55 (2019) 140.
- [16] V. Caracciolo et al., Search for  $\alpha$  decay of naturally occurring Hf-nuclides using a  $\text{Cs}_2\text{HfCl}_6$  scintillator, *Nucl. Phys. A* 1002 (2020) 121941.
- [17] W. Porschen, W. Riezler, Sehr langlebige natürliche  $\alpha$ -Strahler, *Z. Naturforsch.* 11 (1956) 143.
- [18] C.M. Baglin, Nuclear Data Sheets for  $A = 184$ , *Nucl. Data Sheets* 111 (2010) 275.
- [19] R.F. Sperlein, R.L. Wolke, A search for alpha instability in  $^{184}\text{Os}$ , *J. Inorg. Nucl. Chem.* 38 (1976) 27.
- [20] S.T.M. Peters et al., Alpha-decay of  $^{184}\text{Os}$  revealed by radiogenic  $^{180}\text{W}$  in meteorites: Half life determination and viability as geochronometer, *Earth and Planetary Sci. Lett.* 391 (2014) 69.
- [21] V.E. Viola et al., Alpha decay of natural  $^{186}\text{Os}$ , *J. Inorg. Nucl. Chem.* 37 (1975) 11.
- [22] M. Wang et al., The AME2016 atomic mass evaluation (II). Tables, graphs and references, *Chin. Phys. C* 41 (2017) 030003.
- [23] D.N. Poenaru, M. Ivascu, Estimation of the alpha decay half-lives, *J. Physique* 44 (1983) 791.
- [24] B. Buck, A.C. Merchant, S.M. Perez, Ground state to ground state alpha decays of heavy even-even nuclei, *J. Phys. G* 17 (1991) 1223.
- [25] B. Buck, A.C. Merchant, S.M. Perez, Favoured alpha decays of odd-mass nuclei, *J. Phys. G* 18 (1992) 143.
- [26] P. Belli et al., First search for double- $\beta$  decay of  $^{184}\text{Os}$  and  $^{192}\text{Os}$ , *Eur. Phys. J. A* 49 (2013) 24.
- [27] P. Belli et al., First search for double beta decay of osmium by low background HPGe detector, *Proc. of 4-th Int. Conf. on Current Problems in Nucl. Phys. and At. Energy (NPAE-Kyiv2012)*, Kyiv, 2013, p. 357.
- [28] E.A. McCutchan, Nuclear Data Sheets for  $A = 180$ , *Nucl. Data Sheets* 126 (2015) 151.
- [29] Balraj Singh, Nuclear Data Sheets for  $A = 182$ , *Nucl. Data Sheets* 130 (2015) 21.
- [30] C.M. Baglin, Nuclear Data Sheets for  $A = 183$ , *Nucl. Data Sheets* 134 (2016) 149.
- [31] S.-C. Wu, Nuclear Data Sheets for  $A = 185$ , *Nucl. Data Sheets* 106 (2005) 619.
- [32] C.M. Baglin, Nuclear Data Sheets for  $A = 186$ , *Nucl. Data Sheets* 99 (2003) 1.
- [33] F.G. Kondev, S. Juutinen, D.J. Hartley, *Nucl. Data Sheets* 150 (2018) 1.
- [34] V.M. Azhazha, G.P. Kovtun, G.F. Tihinsky, The obtaining and metallophysics of high-pure metals, *Metallofizika i Noveishie Tekhnologii* 22 (2000) 21 (in Russian).

- [35] W.M. Haynes (ed), *CRC Handbook of Chemistry and Physics*, 97th Edition. (CRC Press. Boca Raton, Florida 2017).
- [36] S.B. Shirey, R.J. Walker, Carius Tube Digestion for Low-Blank Rhenium-Osmium Analysis, *Anal. Chem.* 67 (1995) 2136.
- [37] A.S. Cohen, F.G. Waters, Separation of osmium from geological materials by solvent extraction for analysis by thermal ionisation mass spectrometry, *Anal. Chim. Acta* 332 (1996) 269.
- [38] J.L. Birck, M.R. Barman, F. Capmas, Re-Os Isotopic Measurements at the Femtomole Level in Natural Samples, *Geostandard Newslett.* 20 (1997) 19.
- [39] J.L. Birck, The Precision and Sensitivity of Thermal Ionisation Mass Spectrometry (TIMS): An Overview of the Present Status, *Geostandard Newslett.* 25 (2001) 253.
- [40] A.O. Nier, The isotopic constitution of osmium. *Phys. Rev.* 52 (1937) 885.
- [41] D. Selby, R.A. Creaser, Re-Os geochronology of organic rich sediments: an evaluation of organic matter analysis methods, *Chem. Geol.* 200 (2003) 225.
- [42] J. Völkening, T. Walczyk, K.G. Heumann, Osmium isotope ratio determinations by negative thermal ionization mass spectrometry, *Int. J. Mass Spectrom. Ion Proc.* 105 (1991) 145.
- [43] J. Meija et al., Isotopic compositions of the elements 2013 (IUPAC Technical Report), *Pure Appl. Chem.* 88 (2016) 293.
- [44] Z. Zhu et al., Determination of the isotopic composition of osmium using MC-ICPMS, *Anal. Chem.* 90 (2018) 9281.
- [45] M. Laubenstein, Screening of materials with high purity germanium detectors at the Laboratori Nazionali del Gran Sasso, *Int. J. Mod. Phys. A* 32 (2017) 1743002.
- [46] S. Agostinelli et al., GEANT4—a simulation toolkit, *Nucl. Instrum. Meth. A* 506 (2003) 250.
- [47] J. Allison et al., Geant4 developments and applications, *IEEE Trans. Nucl. Sci.* 53 (2006) 270.
- [48] M. Boswell et al., MaGe-a Geant4-Based Monte Carlo Application Framework for Low-Background Germanium Experiments, *IEEE Trans. Nucl. Sci.* 58 (2011) 1212.
- [49] I. Kawrakow, D.W.O. Rogers, The EGSnrc code system: Monte Carlo simulation of electron and photon transport, NRCC Report PIRS-701, Ottawa, 2003.
- [50] G.J. Feldman, R.D. Cousins, Unified approach to the classical statistical analysis of small signals, *Phys. Rev. D* 57 (1998) 3873.
- [51] R.D. Cousins, V.L. Highland, Incorporating systematic uncertainties into an upper limit, *Nucl. Instrum. Meth. A* 320 (1992) 331.

- [52] K. Heyde, *Basic Ideas and Concepts in Nuclear Physics*, 2nd ed. (IoP Publ., Bristol, 1999).
- [53] F.A. Danevich et al.,  $\alpha$  activity of natural tungsten isotopes, *Phys. Rev. C* 67 (2003) 014310.
- [54] C. Cozzini et al., Detection of the natural  $\alpha$  decay of tungsten, *Phys. Rev. C* 70 (2004) 064606.
- [55] A. Munster et al., Radiopurity of  $\text{CaWO}_4$  crystals for direct dark matter search with CRESST and EURECA, *JCAP* 05 (2014) 018.
- [56] Yu.G. Zdesenko et al., Scintillation properties and radioactive contamination of  $\text{CaWO}_4$  crystal scintillators, *Nucl. Instrum. Meth. A* 538 (2005) 657.
- [57] P. Belli et al., Radioactive contamination of  $\text{ZnWO}_4$  crystal scintillators, *Nucl. Instrum. Meth. A* 626-627 (2011) 31.
- [58] P. Belli et al., Search for  $\alpha$  decay of natural Europium, *Nucl. Phys. A* 789 (2007) 15.
- [59] N. Casali et al., Discovery of the  $^{151}\text{Eu}$   $\alpha$  decay, *J. Phys. G* 41 (2014) 075101.
- [60] P. Belli et al., First observation of  $\alpha$  decay of  $^{190}\text{Pt}$  to the first excited level ( $E_{exc} = 137.2$  keV) of  $^{186}\text{Os}$ , *Phys. Rev. C* 83 (2011) 034603.
- [61] R.D. Macfarlane, T.P. Kohman, Natural alpha radioactivity in medium-heavy elements, *Phys. Rev.* 121 (1961) 1758.